ACTA CHEMICA SCANDINAVICA 22 (1968) 1004–1012

The Phase Diagram of the System Na_3AlF_6-CaF_2, and the Constitution of the Melt in the System

JAN LÜTZOW HOLM

Institute of Inorganic Chemistry, The Technical University of Norway, Trondheim, Norway

The system cryolite-calcium fluoride has been examined in the composition range from 0 to 90 mole % CaF_2 by thermal analysis, differential thermal analysis, and equilibration followed by quenching and identification of quenched samples by X-ray diffraction technique and optical microscopy.

The system is a simple eutectic quasi-binary system. No solid solubility was found on either side. An eutectic point was established at 50.0 mole % (27.1 weight %) calcium fluoride and 945.5°C.

The molten mixture of cryolite and calcium fluoride is treated as a regular mixture. By assuming random distribution of Ca^{2+} over the Al^{3+} positions and by using an interaction parameter $b = +1200 \pm 300$ cal, it is possible to rationalize the liquidus line on the cryolite side fairly well. Measurements of enthalpies of solution of CaF_2 in molten cryolite at 1014°C confirm the suggested model, and the positive heat of mixing.

I. INTRODUCTION

The phase diagram of the system cryolite-calcium fluoride was examined for the first time by Pascal [1] in 1913. Later the system has been reexamined by Fenerty and Hollingshead [2] and Matiasovsky and Malinovsky.[3] These diagrams, however, were mainly the results of cooling curve studies and concerned with establishing the liquidus line more precisely. Therefore, they contain very little information about the solidus line. The phase diagram of Pascal [1] (reprinted in Phase Diagrams for Ceramists [4]), indicate a considerable solid solubility on both sides of the system. Recently a work by Rolin,[5] indicating a solubility of about 20 weight % CaF_2 in solid cryolite at 940°C has been published. The solid solubility, however, seems to decrease very rapidly with the temperature. Rolin suggested at the same time that the system should be examined by other methods before the phase relations could be definitely established.

In this work the following methods have been used to determine the liquidus and solidus curves in the system: thermal analysis, differential thermal analysis, quenching technique with microscopic and X-ray investigations of quenched samples, and density measurements of samples of different compositions.

II. EXPERIMENTAL

1) *Chemicals.* The cryolite was handpicked, natural cryolite from Ivigtut, Greenland, melting point 1010.8°C. Calcium fluoride, CaF_2 a.r. grade, from Mallinckrodt Chemical Works, USA, was dried at 400°C in a vacuum furnace before use.

2) *Thermal analysis.* The equipment used for the cooling curve work in the present study have been described in previous papers.[6,7] Supercooling of the melt was prevented by stirring as well as seeding with small crystals of cryolite. Two thermal arrests in the cooling curves were recorded (the liquidus and the solidus curve). During some of the runs also the transition temperature for the conversion of β-cryolite to the low temperature α-modification was recorded.

3) *Differential thermal analysis.* Samples of different compositions were also examined by differential thermal analysis. The cooling curves were recorded by a Speedomax G X-Y recorder and by use of a D. C. Microvolt Amplifier (range 50—2000 microvolt, Leeds and Northrup, USA).

4) *Quenching experiments.* The technique of quenching after equilibration of samples at predetermined temperatures was used in several ways to supplement the information obtained by thermal analysis. Liquids in the system could not be quenched to glasses, instead a complex of very fine crystals was obtained. Fused samples were put into small platinum capsules and heated in the furnace to 940 and 950°C. After equilibration for 1—2 h, the samples were quenched in oil, ground to assure homogeneity, and examined by both X-ray diffraction and optical microscopy.

a) X-Ray diffraction. Routine X-ray analysis for identification of phases in quenched samples were made by using a Nonius type Guinier Camera and Cu$K\alpha$-radiation.

b) Optical microscopy. A petrographic microscope was used for identification of the phases present in the system. The identification was based on optical properties reported by Kordes.[8]

5) *Density measurements.* The density measurements were carried out at 25°C by a vacuum pycnometric method using Shell Odourless Kerosene as a displacement liquid.

III. RESULTS

Results obtained by thermal analysis (cooling curve method) are listed in Table 1 and plotted in a phase diagram in Fig. 1. At regular cooling rates

Table 1. System Na_3AlF_6—CaF_2. Results from thermal analysis.

T_1 = temperature of first crystallization (liquidus curve)
T_2 = second thermal arrest
T_{tr} = cryolite transition temperature

Weight % CaF_2	Mole % CaF_2	T_1°C	T_2°C	T_{tr}°C
0	0	1010.8		560.3
0.51	1.30	1009.3		560.4
0.57	1.52	1008.9		560.3
1.05	2.78	1007.7		560.4
2.03	5.39	1004.6		
3.04	7.77	1001.5		
4.83	12.00	996.5		
9.96	22.89	982.5	922	560.1
16.55	34.78	966.9	935	
20.49	40.97	958.5	939	
27.11	50.00		945.2	
31.28	55.00		945.5	
39.87	64.00		945.1	

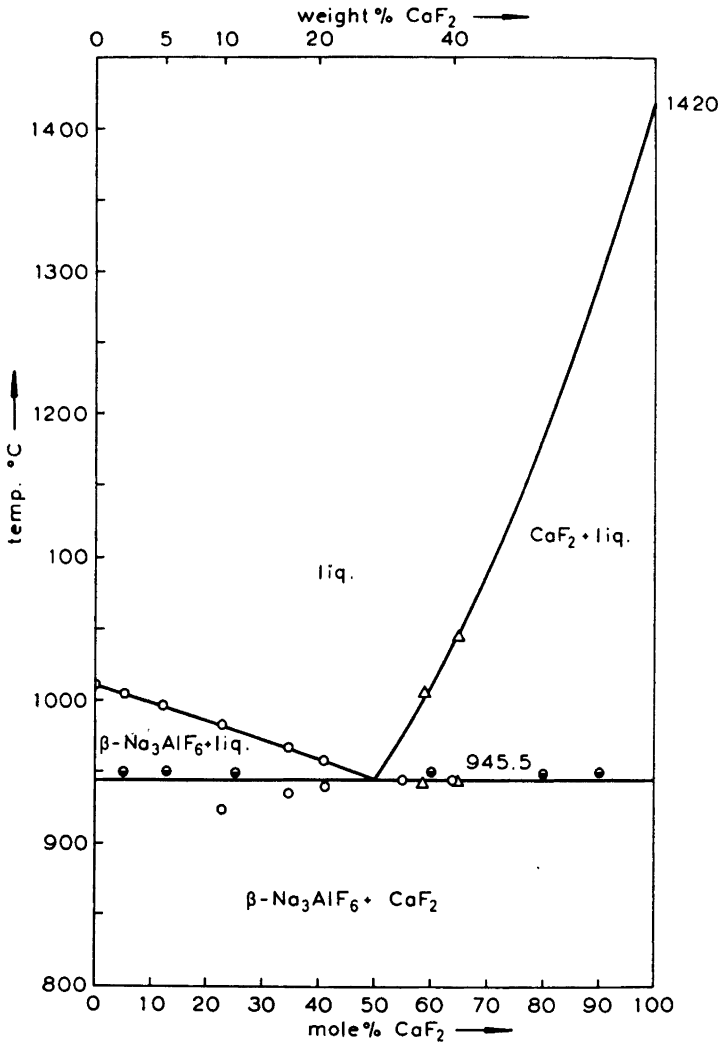

Fig. 1. The phase diagram of the system Na_3AlF_6-CaF_2 from the present work.
O points obtained from thermal analysis, △ points obtained from DTA cooling curves, ◒ points obtained from quenching experiments indicating that one solid phase + a liquid phase are present.

(0.5—1.0°C/min), a real eutectic halt was never observed at the cryolite side of the system. The halts seemed to vary between 922°C for the 23 mole % CaF_2 composition and 945°C for the 50 mole % CaF_2 composition. Similar effects were also observed by DTA examinations of samples of different compositions as shown in Table 2. This can be due to formation of solid solu-

Table 2. Results from DTA examinations. T_1, T_2, and T_3 are first, second, and third thermal arrest.

Composition, mole % CaF_2	T_1°C	T_2°C	T_3°C
9.88	997	—	(785)
19.75	986	913	(782)
20.26	984	917	(781)
54.87	—	946	(785)
59.41	1006	942	(780)
65.02	1046	943	(784)

tions of CaF_2 and Na_3AlF_6 as indicated by Rolin.[5] However, in addition each of the DTA cooling diagrams also contained a small exothermic peak at about 785°C (Fig. 2). This temperature is near the observed eutectic temperature in the ternary system NaF-Na_3AlF_6-CaF_2 reported by Fedotjev.[9]

Thus, the cooling curves indicate that the crystallization ends at the ternary eutectic point of the system NaF-Na_3AlF_6-CaF_2. It is assumed that small amounts of AlF_3 or $NaAlF_4$ will vaporize from the melt at higher temperatures. This will displace the NaF/AlF_3 molar ratio from 3 to a higher value. Particularly with small additions of CaF_2 to the cryolite melt, the ratio NaF (excess)/CaF_2 will be quite conclusive for the depression of the eutectic temperature of the binary system, and the observed second thermal

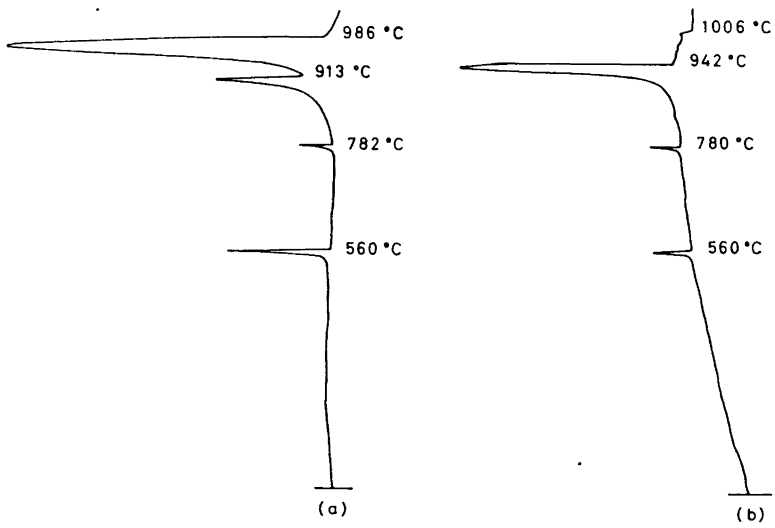

Fig. 2. DTA cooling curves for two of the cryolite-calcium fluoride mixtures.
a) 20 mole % calcium fluoride,
b) 59.4 mole % calcium fluoride.

Fig. 3. Photomicrograph of the cryolite phase in a 5 mole % CaF_2 + 95 mole % Na_3AlF_6 mixture quenched from 950°C showing coexisting primary crystals of cryolite and quenched liquid. Magnification, × 200.

arrest will deviate from the real eutectic temperature, 945°C. However, at higher concentrations of CaF_2 the content of excess NaF in the melt will be of less importance and fairly stable eutectic temperatures are observed from 35 to 64 mole % CaF_2. The results from the microscopic examinations of samples containing from 5 to 90 mole % CaF_2 and quenched from 950°C, showed the presence of primary crystals of either Na_3AlF_6 or CaF_2 in equilibrium with quenched liquid (see Fig. 3). This indicates that there is no formation of solid solution in the system between 5 and 90 mole % CaF_2.

The densities of samples quenched from 970°C are given in Table 3 together with the calculated densities of mechanical mixtures of Na_3AlF_6 and CaF_2. The following densities have been used for Na_3AlF_6, $d = 2.959$ g/cm³ (Holm [7]), and for CaF_2, $d = 3.18$ g/cm³ (Swanson and Tatge [10]). The observed and calculated densities compare very favourably as can be seen from Table 3.

It is therefore assumed that the system Na_3AlF_6-CaF_2 constitutes a simple quasi-binary eutectic system with no solid solubility on either side of the system. The eutectic point is established at 50 mole % CaF_2 and 945.5.°C.

Table 3. Densities in g/cm³ of samples quenched from above the liquidus temperature.

Weight %	Mole %	Quenching Temp. °C	Densities g/cm³	
			Observed	Calculated, mechanical mixture
5	12.5	970	2.968	2.970
10	23	970	2.984	2.980
35	60	970	3.034	3.033

IV. STRUCTURAL PROPERTIES OF MOLTEN MIXTURES OF CRYOLITE AND CALCIUM FLUORIDE

In the electrolytic production of aluminium the electrolyte consists of a solution of about 3 to 8 weight % alumina in cryolite with a small excess of aluminium fluoride. Some plants also operate with additions of 5 to 10 weight % calcium fluoride to lower the melting point of the bath, although it is well known that calcium fluoride also decreases the electrical conductivity (Abramov [11] and Yim and Feinleib [12]) and increases the density (Belyaev [13]).

It should be noted that very often the added alumina contains traces of calcium oxide. The calcium oxide reacts with the cryolite or the aluminium fluoride to form calcium fluoride and alumina according to the reactions

$$2Na_3AlF_6 + 3\,CaO = 6\,NaF + 3\,CaF_2 + Al_2O_3 \quad (1)$$

$$2\,AlF_3 + 3\,CaO = 3\,CaF_2 + Al_2O_3 \quad (2)$$

It is believed that since the Na^+ and Al^{3+} ions are so different with respect to size and charge, they cannot easily exchange positions with each other in the melt. The pure molten cryolite lattice is then supposed to consist of two different types of cation positions, Na^+ and Al^{3+}, and one type of anion position, F^-. By addition of CaF_2 to molten cryolite it is most likely that Ca^{2+} will prefer Na^+-ions as next nearest neighbours, and that a Ca^{2+}-ion therefore will take a Al^{3+} position in the melt as indicated by the reaction:

$$\begin{array}{c} F^- \\ Na^+F^-Al^{3+}F^-Na^+F^- \\ F^- \end{array} \begin{array}{c} F^- \\ Al^{3+}F^-Na^+ \\ F^- \end{array} + CaF_2 \rightarrow \begin{array}{c} F^- \\ Na^+F^-Al^{3+}F^-Na^+F^- \\ F^- \end{array} \begin{array}{c} F^- \\ Ca^{2+}F^-Na^+ \\ F^- \end{array} \quad (3)$$

In a mixture of n_1 mole Na_3AlF_6 and n_2 mole CaF_2 the mole fractions of the two components will be given by:

$$N_{Na_3AlF_6} = \frac{n_1}{n_1 + n_2} \qquad \text{and } N_{CaF_2} = \frac{n_2}{n_1 + n_2}$$

The excess partial free energy of cryolite can be expressed by

$$\bar{G}^e_{Na_3AlF_6} = b \cdot N^2_{CaF_2} \quad (4)$$

where b is a function of the mole fraction N_{CaF_2}. The excess partial free energy can be calculated from the observed freezing point depressions by using the relation

$$\bar{G}^e_{Na_3AlF_6} = -\Delta H_f\left(1 - \frac{T}{T_f}\right) + \frac{\Delta Cp}{2}\frac{(\Delta T)^2}{T} - RT \ln N_{Na_3AlF_6} \quad (5)$$

Here ΔH_f is the heat of fusion of cryolite, $\Delta H_f = 27.64$ kcal/mole (O'Brien and Kelley [14]). ΔCp is the difference in specific heat of the pure liquid and pure solid cryolite. $\Delta T = T_f - T$, where T is the melting temperature of the mixture. The best fit for $\bar{G}^e_{Na_3AlF_6}/N^2_{CaF_2}$ is obtained by the relation:

$$\bar{G}^e/N^2_{CaF_2} = 690 + 410\,N_{CaF_2} + 1555\,N^2_{CaF_2} \quad (6)$$

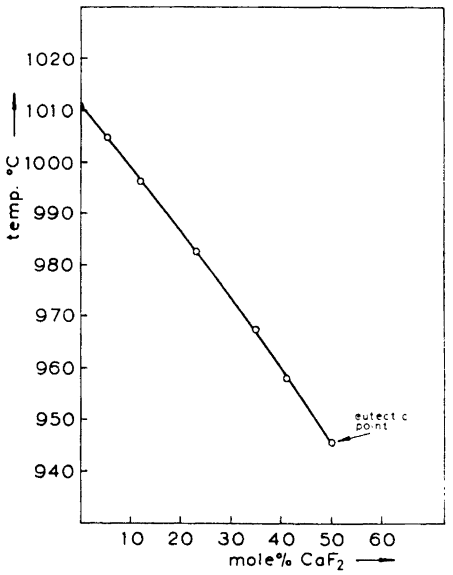

Fig. 4. The liquidus curve on the cryolite side of the phase diagram $Na_3AlF_6-CaF_2$. Circles represent observed points from the present work. The solid line is calculated by assuming regular solution, $b = +1000 \pm 300$ cal, and random distribution of Ca^{2+} ions and Al^{3+} positions.

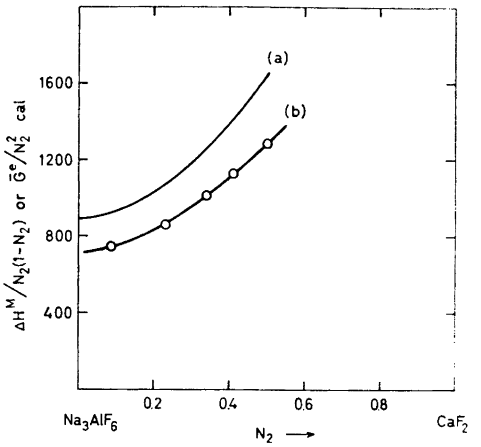

Fig. 5. $\Delta H^M/N_2(1 - N_2)$, curve (a), and $\overline{G}_1^e/N_2^2$, curve (b), as a function of mole fraction calcium fluoride, N_2.

The mixture can as a first approximation be treated as a strictly regular solution. By choosing a value of approximately +1000 cal for the interaction parameter b in eqn. (4), it is possible to rationalize the liquidus line fairly well as shown on Fig. 4. The activity of cryolite in mixtures of calcium fluoride can then easily be calculated from the expression:

$$RT \ln a_{Na_3AlF_6} = (1000 \pm 300) N^2_{CaF_2} + RT \ln N_{Na_3AlF_6} \quad (7)$$

The calorimetrically determined heat of fusion of calcium fluoride as given by Naylor [15] is 7100 cal/mole at the melting point, 1691°K. According to Naylor calcium fluoride also undergoes a second order phase change at 1424°K. From Naylor's values of heat capacities for the solids and the liquid phase the heat of fusion at 1287°K is calculated as 8900 cal/mole.

Enthalpies of solution of calcium fluoride in molten cryolite at 1287°K have been determined by solution calorimetry (Holm [16]). A constant value of 9.7 ± 0.3 kcal/mole was obtained for mixtures containing from 0 to 10 mole % CaF_2. Assuming that the heat of solution of CaF_2 is independent of composition, one obtains for the function $\Delta H^M/(1 - N_{CaF_2}) N_{CaF_2}$

$$\Delta H^M/(1 - N_{CaF_2}) N_{CaF_2} = 890 + 230 N_{CaF_2} + 2500 N^2_{CaF_2} \quad (8)$$

This curve is plotted on Fig. 5 (a) and should be compared with the free energy curve (b) obtained by plotting $\bar{G}^e/N^2_{CaF_2}$. Assuming as for the free energy, eqn. (6), that the heat of mixing as a first approximation can be expressed by a simple regular solution equation, one obtains

$$\Delta H^M = (1200 \pm 400)\, N_{CaF_2}\,(1 - N_{CaF_2}) \qquad (9)$$

or for the partial enthalpy of mixing for cryolite

$$\Delta \bar{H}_{Na_3AlF_6} = (1200 \pm 400)\, N^2_{CaF_2} \qquad (10)$$

Positive excess entropies are found as given by the difference between eqn. (10) and eqn. (7).

$$T\bar{S}^e_{Na_3AlF_6} = (200 \pm 500)\, N^2_{CaF_2} \qquad (11)$$

At the 50:50 composition the excess partial molar entropy is $\bar{S}^e = +0.04 \pm 0.09$ e.u. as compared to the total partial configurational entropy for cryolite $\Delta\bar{S}_{conf} = 1.38$ e.u.

Here it should be added that the adopted model does not take into account a partial dissociation of the cryolite anion. Grjotheim [6] has suggested that the cryolite anion dissociated partially according to

$$AlF_6^{3-} = AlF_4^- + 2F^-$$

with a dissociation constant, $K = 0.06$.

A dissociation of the anion as illustrated above, should give an extra contribution to the configurational entropy. Hence, one would expect to observe a positive excess entropy. It is, however, difficult to make a quantitative estimate of the degree of dissociation from the observed excess entropies as given by eqn. (9), since other types of entropies like vibrational entropy, may as well contribute to the total entropy of mixing.

Finally, it should be added that in the case of acid electrolytes, *i.e.* Na_3AlF_6-AlF_3 mixtures, the discussion of the structural properties of the molten mixture will be more intricate. It may now be possible for the Ca^{2+}-ions to a larger extent to exchange positions with Na^+-ions, and to participate in the conductivity process as indicated by the conductivity measurements by Yim and Feinleib.[12]

Acknowledgement. The author acknowledges his indebtedness to Professor K. Grjotheim and to the *Royal Norwegian Council for Scientific and Industrial Research* for financial support.

REFERENCES

1. Pascal, P. *Z. Electrochem.* **19** (1913) 611.
2. Fenerty, A. and Hollingshead, E. A. *J. Electrochem. Soc.* **107** (1960) 993.
3. Matiasovsky, K. and Malinovsky, M. *Chem. Zvesti* **14** (1960) 253.
4. Levin, E. M. *Phase Diagrams for Ceramists*, The American Ceramic Society, Ohio, USA 1964, p. 445.
5. Rolin, M. *Bull. Soc. Chim. France* **1961** 1120.
6. Grjotheim, K. *Contributions to the Theory of Aluminium Electrolysis, Kgl. Norske Videnskab. Selskabs, Skrifter* **1956** No. 5.

7. Holm, J. L. *Undersøkelser av struktur og faseforhold for en del systemer med tilknytning til aluminiumelektrolysen*, Lic. Thesis. Institute of Inorganic Chemistry, The Technical University of Norway 1963.
8. Kordes, E. *Optische Daten*, Verlag Chemie, Weinheim 1961.
9. Fedotiev, P. P. and Iljinsky, W. P. *Z. anorg. allgem. Chem.* **129** (1923) 106.
10. Swanson, H. E. and Tatge, E. *Standard X-ray Diffraction Patterns, J. Res. Natl. Bur. Std.* **46** (1951) 318.
11. Abramov, G. A. *The Basic Theory of the Electrometallurgy of Aluminium*, Metallurg. Moscow 1953, p. 532 (in Russian).
12. Yim, E. W. and Feinleib, M. *J. Electrochem. Soc.* **104** (1957) 626.
13. Belyaev, A. I. *Metallurgie des Aluminiums*, VEB Verlag Technik, Berlin 1956.
14. O'Brien, C. J. and Kelley, K. K. *J. Am. Chem. Soc.* **79** (1957) 5116.
15. Naylor, B. F. *J. Am. Chem. Soc.* **67** (1965) 150.
16. Holm, J. L. *Acta Chem. Scand.* **21** (1967) 2292.

Received October 16, 1967.